Lipid-Specific Membrane Activity of Human β-Defensin-3†

Arne Böhling,‡ Sven O. Hagge,‡ Stefanie Roes,‡ Rainer Podschun,§ Hany Sahly,§ Jürgen Harder,∥ Jens-Michael Schröder,∥ Joachim Grötzinger,⊥ Ulrich Seydel,‡ and Thomas Gutsmann*,‡

Department of Immunochemistry and Biochemical Microbiology, Leibniz-Center for Medicine and Biosciences, Research Center Borstel, Parkallee 1-40, D-23845 Borstel, Germany, Department of Medical Microbiology and Virology and Clinical Research Unit at the Department of Dermatology, University Hospital Schleswig-Holstein, Campus Kiel, D-24105 Kiel, Germany, and Department of Biochemistry, Christian-Albrechts-Universität zu Kiel, Olshausenstrasse 40, D-24098 Kiel, Germany

Received October 6, 2005; Revised Manuscript Received March 8, 2006

ABSTRACT: Defensins represent a major component of innate host defense against bacteria, fungi, and enveloped viruses. One potent defensin found, e.g., in epithelia, is the polycationic human β-defensin-3 (hBD3). We investigated the role of the lipid matrix composition, and in particular the presence of negatively charged lipopolysaccharides (LPS) from sensitive (*Escherichia coli*, *Salmonella enterica* serovar Minnesota) or resistant (*Proteus mirabilis*) Gram-negative bacteria or of the zwitterionic phospholipids of human cells, in determining the action of polycationic hBD3 on the different membranes, and related to their biological activity. The main focus was directed on data derived from electrical measurements on a reconstitution system of the OM as a planar asymmetric bilayer composed on one side of LPS and on the other of a phospholipid mixture. Our results demonstrate that the antimicrobial activity and the absence of cytotoxicity can be explained by the lipid-specificity of the peptide. A clear correlation between these aspects of the biological activity of hBD3 and its interaction with lipid matrices could be found. In particular, hBD3 could only induce lesions in those membranes resembling the lipid composition of the OM of sensitive bacterial strains. The permeation through the membrane is a decisive first step for the biological activity of many antimicrobial peptides. Therefore, we propose that the lipid-specificity of hBD3 as well as some other membrane-active antimicrobial peptides is important for their activity against bacteria or mammalian cells.

The endogenous immune barrier of mammals against invading microbes provides a number of effective antimicrobial peptides/proteins (AMPs[1]) which are synthesized and active in different compartments (*1*). These peptides include those of the granulocytes, e.g., the bactericidal/permeability increasing protein (BPI), cathelicidins, and neutrophilic defensins (for reviews see refs *2*−*5*), and of the epithelia, e.g., psoriasin (*6*), β-defensins (*7*), and cathelicidins (*8*).

AMPs that contain six cysteines in intramolecular disulfide linkage have been classified as defensins. They are divided into four different groups, α-, β-, θ-, and insect defensins due to the connectivity of the cysteines (for reviews see refs *9*, *10*). The first isolated human β-defensin (hBD1) was purified from hemofiltrates (*11*); the second and third (hBD2 and hBD3, respectively) were discovered in extracts of lesional scales from patients suffering from psoriasis (*12*−*14*). By screening the human genome database, a further member of the hBD family, the hBD4, was identified (*15*). The β-defensins contain 38−45 amino acids and are 1−5, 2−4, 3−6 disulfide-linked (*16*). hBD3 is composed of 45 amino acids and exhibits in solution a β-sheet structure (*17*). The overall net charge is +11 e_0.

hBD3 is produced by, e.g., keratinocytes and lung epithelial cells and exhibits a broad spectrum of antimicrobial activity in vitro against Gram-positive bacteria (*Staphylococcus aureus* and *Streptococcus pyogenes*), fermentative and nonfermentative Gram-negative bacteria (*Pseudomonas aeruginosa* and *Escherichia coli*), and the yeast *Candida albicans*. However, some species, such as *Burkholderia*, are highly resistant (*18*). Up to 500 μg/mL no significant hemolytic activity of hBD3 was observed at physiological salt concentrations (*14*).

In earlier studies, we found that the sensitivity or resistance of certain Gram-negative strains from various species as well as the sensitivity of eukaryotic cells against polymyxin B (PMB), fragments of rabbit and human 18 kDa cationic antimicrobial protein (CAP18, LL37), and BPI is correlated with the lipid-specific interaction with and/or induction of

† This study was supported by the Deutsche Forschungsgemeinschaft (SFB 617).

* Author to whom correspondence should be addressed. Mailing address: Research Center Borstel, Parkallee 1-40, D-23845 Borstel, Germany. Tel: +49-(0)4537-188 291. Fax: +49-(0)4537-188 632. E-mail: tguts@fz-borstel.de.

‡ Research Center Borstel.

§ Department of Medical Microbiology and Virology, University Hospital Schleswig-Holstein.

∥ Clinical Research Unit at the Department of Dermatology, University Hospital Schleswig-Holstein.

⊥ Christian-Albrechts-Universität zu Kiel.

[1] Abbreviations: AMP, antimicrobial peptide; BPI, bactericidal/permeability increasing protein; hBD, human β-defensin; PMB, polymyxin B; CAP18, 18 kDa cationic antimicrobial protein; OM, outer membrane; LPS, lipopolysaccharide; PL, phospholipid mixture; LB, Langmuir−Blodgett; AFM, atomic force microscope; ReLPS, deep rough mutant LPS; Ara4N, 4-amino-4-deoxyarabinose; Kdo, 3-deoxy-D-*manno*-oct-2-ulosonic acid; PE, phosphatidylethanolamine; PG, phosphatidylglycerol; PC, phosphatidylcholine; PS, phosphatidylserine; DPG, diphosphatidylglycerol; MBC, minimal bactericidal concentration; LE, liquid expanded; LC, liquid condensed.

10.1021/bi052026e CCC: $33.50
Published on Web 04/06/2006

lesions in models for the respective membranes (*19*−*23*). According to these findings we hypothesize that lipid-specific interactions of AMPs with membranes are the first step determining their biological activities. The three-dimensional structure of defensins is very different as compared to the structure of PMB, CAP18, and LL37. Thus, a different interaction mechanism for hBD3 is likely to be expected. However, for all AMPs either the permeabilization of the membrane or the passage through the membrane to reach the locus of killing is essential, except for those AMPs which interfere with cell wall biosynthesis, e.g., type B lantibiotics (for review see ref *24*).

The first target for AMPs is, in the case of Gram-negative bacteria, the outer membrane (OM) (*25*). This OM is an asymmetric bilayer with respect to the lipid composition. Incorporated into this lipid matrix are the so-called outer membrane proteins, e.g., the porins, which have a sievelike function for the transport or exclusion of hydrophilic substances; however, their pore sizes are too small to allow the passage of hBD3. The outer leaflet consists generally of lipopolysaccharide (LPS) (*26*) and the inner leaflet of a phospholipid mixture (PL) (*27*). LPS carries negatively charged groups resulting in a negative surface charge density of the outer leaflet of the OM, and, thus, an electrostatic interaction between LPS and the polycationic hBD3 is likely.

In the present study, we investigated whether the resistance or sensitivity of certain Gram-negative species and the noncytotoxicity against eukaryotic cells against hBD3 can be explained by the lipid composition of the respective membranes to verify the hypothesis formulated above. To this end, we performed bacteria killing assays as well as measurements on membrane reconstitution systems using the isolated LPS of the respective strains. As the most simplified model for membranes we used lipid monolayers to characterize their interaction with hBD3. We allowed hBD3 to intercalate into LPS and phospholipid monolayers, prepared them as solid supported Langmuir−Blodgett (LB) films (*28*), and imaged them with an atomic force microscope (AFM). We found an intercalation of hBD3 as well as hBD3-induced changes in the domain structure only of LPS monolayers resembling the OM of the sensitive strains.

To get further insight into the peptide-induced permeabilization and destabilization of lipid membranes, the planar lipid bilayers are a powerful tool (*21*, *29*, *30*). Using the Montal−Mueller method (*31*) it is possible to reconstitute even the asymmetric OM of Gram-negative bacteria (*32*). Adding hBD3 to the LPS side, we observed the formation of voltage-dependent and lipid-specific lesions.

On the basis of our results, our hypothesis that the composition of the lipid matrix determines the antimicrobial activity of hBD3 seems to be verified.

MATERIALS AND METHODS

Lipids and Other Chemicals. For the preparation of reconstituted membranes, deep rough mutant LPS (ReLPS) from *E. coli* strain F515 (LPS F515), *Salmonella enterica* serovar Minnesota strain R595 (LPS R595), and *Proteus mirabilis* strain R45 (LPS R45) (*33*−*38*) were used (Figure 1). LPS was extracted by the phenol/chloroform/petroleum ether method (*39*), purified, lyophilized, and transformed into the triethylamine salt form. The amounts of nonstoichiometric substitutions by fatty acids, 4-amino-4-deoxyarabinose (Ara4N), and phosphoethanolamine were analyzed mass spectrometrically. In LPS R595 and LPS R45, the phosphates linked to the 4′-phosphate on the second glucosamine were found to be substituted with Ara4N by approximately 40% and 50%, respectively. In LPS R45, also approximately 50% of the first 3-deoxy-D-*manno*-oct-2-ulosonic acid (Kdo) is substituted with Ara4N.

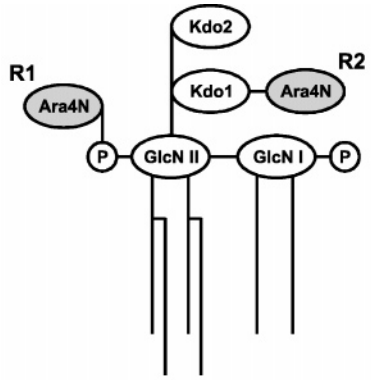

	LPS F515	LPS R595	LPS R45
R1	0 %	65 %	50 %
R2	0 %	0 %	50 %
Charge / e_0	-4	-3.4	-3

FIGURE 1: Structure of various LPS utilized in this study. Structures of deep-rough mutant LPS from *E. coli* strain F515, *S. enterica* sv. Minnesota strain R595, and *P. mirabilis* strain R45 are shown. Negative and positive charges are indicated. The amounts of nonstoichiometric substitutions by Ara4N and the net negative charges are given in the table. The fatty acid substitutions resemble the natural mixtures in each case (*37*).

Phosphatidylethanolamine (PE) from *E. coli*, phosphatidylglycerol (PG) from egg yolk lecithin, phosphatidylcholine (PC) from chicken egg, phosphatidylserine (PS) from porcine brain, and synthetic diphosphatidylglycerol (DPG) and diphytanoylphosphatidylcholine were purchased from Avanti Polar Lipids (Alabaster, AL) and used without further purification.

Synthetic hBD3 was obtained from Jerini Bio Tools GmbH (Berlin, Germany), and recombinant hBD3 was produced as described earlier. Both were analyzed mass spectrometrically and showed identical antimicrobial activity as compared to the naturally derived peptide (*14*). hBD3 was dissolved in 0.01% acetic acid.

Antimicrobial Assay. Bacteria were grown for 2 to 3 h in brain heart infusion broth at (36 ± 1) °C. The bacteria were washed three times in 10 mM sodium phosphate buffer at pH 7.4, and adjusted to a concentration of 10^4 to 10^5 bacteria/mL. One hundred microliters of this solution was mixed with 10 μL of hBD3 solution (the maximum concentration used was 100 μg/mL) and incubated at (36 ± 1) °C for 2 h, and the colony forming units were determined. The negative control was supplemented with 10 μL of phosphate buffer or with 10 μL of 0.01% acetic acid instead of hBD3. Results are given as minimal bactericidal concentrations (MBC, ≥99.9% killing).

Film Balance Measurements and Atomic Force Microscopy of Langmuir−Blodgett Films. Using a film balance, monolayers prepared at the air/water interface can be compressed, and the lateral pressure in dependence on the

surface area can be recorded. The intercalation of hBD3 into monolayers was studied using monolayers spread from 4 μL of a 1 mM chloroform/methanol (9:1 v/v) solution of LPS or 2.3 μL of a 3.3 mM chloroform solution of PC. The experiments were run at 20 °C to achieve a stable transfer of the monolayers onto mica for AFM experiments. Prior to isotherm recording, monolayers were equilibrated at zero pressure for 7 min to allow evaporation of the solvent. The monolayers were then compressed to a lateral pressure of 20 mN/m, which is in the range of the values discussed for the lateral pressure in cell membranes (*40*). The LPS monolayers were equilibrated for 1 h at constant lateral pressure. Fifty microliters of a 0.1 mg/mL solution of hBD3 was injected into 80 mL of subphase (5 mM HEPES, pH 7), and changes in film area versus time were plotted for 1 h.

For AFM measurements, monolayers were transferred to mica plates according to the LB technique (*28*) with a pulling speed of 10 μm/s and the monolayers were imaged under atmospheric conditions (in air) with the MFP3D (Asylum Research, Santa Barbara, CA) in contact (DC, dragging) mode using cantilever E of the MSCT-AUNM with a typical spring constant of 100 mN/m and a resonance frequency of 34 kHz (Park Scientific Instruments/Veeco, Santa Barbara, CA).

Preparation of Planar Bilayers and Electrical Measurements. Planar bilayers were prepared according to the Montal−Mueller technique (*31*) as described earlier (*41*). Briefly, symmetric and asymmetric bilayers were formed by opposing two lipid monolayers prepared on aqueous subphases from chloroformic solutions of the lipids at a small aperture (∅ ∼ 150 μm) in a thin Teflon septum. The inner leaflet of the OM of Gram-negative bacteria was reconstituted by a phospholipid mixture (PL) consisting of PE, PG, and DPG (molar ratio 81:17:2) resembling the phospholipid composition of the inner leaflet of the OM of *Salmonella typhimurium* being composed of the same constituents as that of the other strains used (*27*, *42*). For the reconstitution of the cytoplasmic membrane of eukaryotic cells, instead of natural PC, diphytanoylphosphatidylcholine was used to obtain a higher stability of the membranes. For electrical measurements, planar membranes were voltage-clamped via a pair of Ag/AgCl electrodes (type IVM E255, Advanced Laboratory Research Inc., Franklin) connected to the headstage of an L/M-PCA patch-clamp amplifier (List-Medical, Darmstadt, Germany). In all experiments, the compartment to which hBD3 was added is named first, and the compartment opposite to the addition was grounded. Therefore, in comparison to the natural system, a positive clamp voltage represents a membrane which is negative on the inside. All measurements were performed at a temperature of 37 °C with subphases consisting of 100 mM KCl and 5 mM $MgCl_2$ (specific electrical conductivity 17.2 mS/cm) buffered with 5 mM HEPES and adjusted to pH 7. These salt concentrations were chosen to guarantee (i) a sufficient flux of K^+ ions through peptide-induced membrane lesions, resulting in a current significantly higher than the noise, and (ii) a sufficient membrane stability by cross-linking the LPS molecules by Ca^{2+} ions (as in the natural system). In the case of natural membranes, ions can influence the transmembrane potential. However, in the case of planar lipid bilayers the transmembrane potential is applied externally and, thus, ions have no influence.

At the beginning of each experiment, membrane formation was checked by measuring membrane current and capacitance. Only membranes with a basic current of less than ±2.5 pA at clamp voltages of ±100 mV and a capacitance >90 pF were used for the experiments.

Two electrical parameters were determined: (i) current through hBD3-induced lesion and (ii) hBD3-induced changes of the membrane capacitance. The membrane capacitance yields information on area, thickness, and composition of the bilayer (*19*). Using small positive and negative jumps of the clamp voltage, the maximum voltage required to determine membrane capacitance is <1 mV. Therefore, peptide−membrane interaction can be investigated without the influence of a significant external potential. This method allows the determination of changes in membrane capacitance with a precision of <1 pF.

RESULTS[2]

Antimicrobial Activity. Antimicrobial activities were determined for *E. coli* strain F515, *S. enterica* sv. Minnesota strain R595, and *P. mirabilis* strain R45, and the respective MBC values are 0.39 μg/mL, 3.13 μg/mL, and >100 μg/mL.

Film Balance Measurements and Atomic Force Microscopy of Langmuir−Blodgett Films. Film balance experiments were performed to investigate the intercalation of hBD3 into various lipid monolayers prepared of LPS F515, LPS R595, LPS R45, and PC. The addition of 5 μg of hBD3 into the subphase underneath LPS F515 or LPS R595 monolayers at a constant lateral pressure of 20 mN/m led to an increase in the respective film areas. For monolayers prepared from LPS R45 or PC, we did not detect an hBD3-induced increase in film area within 1 h after peptide addition (data not shown).

Subsequently, we prepared LB films from the respective monolayers on mica. The monolayers of the three different LPS were in the coexistence range of liquid expanded (LE, appearing deeper in the AFM images) and liquid condensed (LC) domains; representative images are shown in Figure 2. PC monolayers did not show any domains because all molecules were in the LE phase. The LE domains were smallest in LPS F515 (Figure 2A), larger in the LPS R595 (data not shown), and largest in the LPS R45 monolayers (Figure 2C). In the LC domains, a substructure could be observed possibly originating from inhomogeneities in the fatty acid composition of the LPS.

The interaction of hBD3 with LPS F515 monolayers led to dramatic changes in domain structures (Figure 2B). The phase separation of the LC and the LE domains disappeared nearly completely, and new types of domains could be observed: (i) domains with diameters >100 nm appearing ∼0.3 nm higher than the monolayer and (ii) small domains with diameters of ∼10 nm appearing ∼1 nm higher. These height differences might be influenced by different attractive or repulsive forces between the cantilever tip and the

[2] All results obtained from biophysical techniques underlie statistical variations. For example, lesion formation in bilayer membranes is a statistical process and depends on various physical parameters, such as diffusion time of the peptide to reach the membrane surface or local concentration variations. Also domain formation in monolayers underlies statistical variations. Nevertheless, the results obtained from at least three independent experiments are qualitatively comparable. Thus, in each case only one representative result is shown.

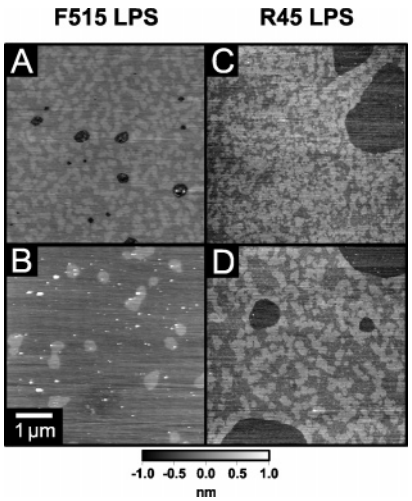

FIGURE 2: Influence of hBD3 on the domain structure of lipid monolayers. AFM images of domain structures of LPS F515 and LPS R45 monolayers in the absence (A and C, respectively) and in the presence (B and D) of hBD3 ([LPS]:[hBD3] = 4:1 M:M) in the subphase prepared as LB films on mica at a lateral pressure of 20 mN/m are shown. The LC domains appear higher than the LE domains. Subphase: 5 mM HEPES, pH 7, $T = 20$ °C.

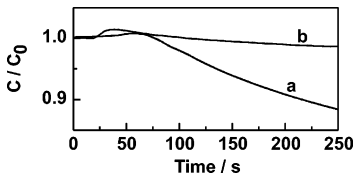

FIGURE 3: Influence of hBD3 on relative membrane capacitance. The membrane capacitances of bilayers in dependence on time after addition of (trace a) 1 μg/mL hBD3 to the LPS side of LPS F515/PL and (trace b) 10 μg/mL hBD3 to PC/PC bilayers were determined in planar bilayer experiments. The PL side consisted of 81 mol % PE, 17 mol % PG, and 2 mol % DPG. Subphase: 100 mM KCl, 5 mM $MgCl_2$, 5 mM HEPES, pH 7, and $T = 37$ °C.

molecules in the different domains. Also in the case of LPS R595 monolayers, changes in domain structure could be observed (data not shown) but not in the case of LPS R45 monolayers (Figure 2D).

Electrical Measurements on Planar Lipid Bilayers. We performed electrical measurements on planar lipid bilayers composed of LPS R595, LPS F515, or LPS R45 on the one and PL on the other side, mimicking the OM of the respective Gram-negative strains used in the antimicrobial assays. Furthermore, we used symmetric PC/PC membranes as a model for the lipid matrix of eukaryotic cells as well as symmetric PS/PS and asymmetric PS/PL bilayers as models for symmetric and asymmetric negatively charged membranes.

In Figure 3 changes in membrane capacitance are depicted exemplarily for LPS F515/PL and PC/PC membranes. The addition of 1 μg/mL hBD3 to membranes, the outer leaflets of which were composed of one of the three different LPS or of PS, led to changes in the capacitance of the respective bilayers of more than 10%, as shown exemplarily for an LPS F515/PL membrane (Figure 3, trace a). These changes occurred in the absence of an externally applied constant clamp voltage. Significant differences between the hBD3-induced capacitance changes in membranes composed of the three LPS could not be observed. Figure 3 shows that even at 10-fold higher hBD3 concentrations the change of the

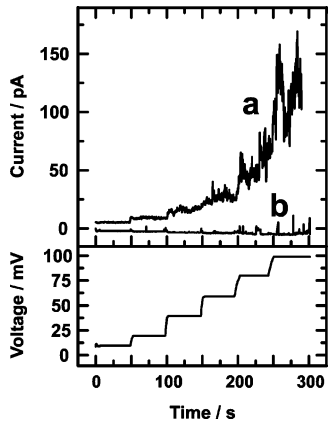

FIGURE 4: Voltage dependence of the induction of lesion formation by hBD3. Upper trace: Voltage-dependent induction of lesion formation after addition of 2 μg/mL hBD3 to the LPS side of LPS F515/PL bilayers (trace a) resembling the OM of a sensitive strain and LPS R45/PL bilayers (trace b) resembling the OM of a resistant strain. Lower trace: Applied clamp voltages. The compositions of the PL side and the subphases were as described for Figure 3.

capacitance of a symmetrical PC/PC bilayer (Figure 3, trace b) is less than 5%. Thus, hBD3 interacts with many types of lipids, however, the changes of the capacitance were more pronounced for negatively charged lipids.

The minimal clamp voltages necessary to induce current fluctuations were investigated by applying different positive and negative clamp voltages. In the case of PL/PL, PS/PS, LPS R595/PL (data not shown), and LPS F515/PL (Figure 4, trace a) membranes, current fluctuations and a general destabilization of the membranes could only be induced at positive clamp voltages. The minimal clamp voltages necessary to induce lesions were $\leq$26 mV, which is the transmembrane voltage across the OM of *E. coli* (*43*). The minimal hBD3 concentration was 1−2 μg/mL. No current fluctuations could be induced in PC/PC (data not shown) and LPS R45/PL (Figure 4, trace b) membranes at clamp voltages between −100 mV and +100 mV and hBD3 concentrations up to 10 μg/mL.

The hBD3-induced current fluctuations showed the following characteristics:

(i) The conductivities and the lifetimes were heterogeneous. For this reason, they were termed lesions rather than pores.

(ii) The lifetimes were in the range of milliseconds.

(iii) The superposition of many single fluctuations led in many cases to a steady state of conductivity for minutes.

(iv) Lesions could only be induced at positive clamp voltages, and the formation rate increased with increasing positive clamp voltages.

(v) At negative clamp voltages, lesions could not be induced, however, lesions which were preformed at positive voltages were stable at least for some time also at negative clamp voltages. In general, negative clamp voltages led to closing of the lesions. This effect could be observed for all types of membranes; it was more pronounced in the case of membranes composed of phospholipids (Figure 6). Whether the absence of a clamp voltage induces closure of lesions is not clear, because in the absence of a clamp voltage the membrane current is zero.

Significant variations in the characteristics of the hBD3-induced lesions, e.g., diameter and lifetime, in PS/PS, LPS

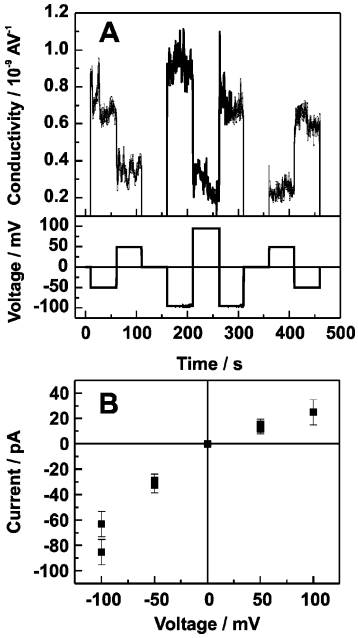

FIGURE 5: Voltage dependence of conductivity and current/voltage characteristics of hBD3-induced lesions in asymmetric LPS/PL membranes. (A) Upper trace: Voltage-dependent conductivity of the lesions in steady state after addition of 2 μg/mL hBD3 to the LPS side of a LPS F515/PL bilayer. Lower trace: Applied clamp voltages. (B) The respective current/voltage characteristics. The compositions of the PL side and the subphases were as described for Figure 3.

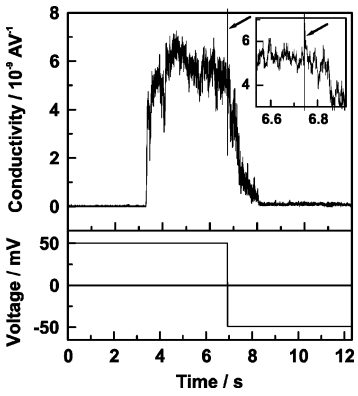

FIGURE 6: Voltage dependence of conductivity of hBD3-induced lesions in symmetric PL/PL membranes. Upper trace: Conductivity of the lesions after addition of 10 μg/mL hBD-3 to a symmetric PL/PL membrane. The inset shows details of the panel at the moment of the voltage step from +50 to −50 mV. Lower trace: Applied clamp voltages. The compositions of PL and the subphases were as described for Figure 3.

R595/PL, and LPS F515/PL membranes could not be observed.

The voltage dependence of the conductivity of the lesions in the steady state was investigated by varying the clamp voltages. In contrast to the formation rate of the lesions, the conductivity in LPS/PL membranes was higher by a factor of ~2 for negative clamp voltages (Figure 5). In phospholipid membranes, for both symmetric PL/PL and asymmetric PS/PL membranes, only the formation rate of the lesions, but not their conductivity, was voltage-dependent (Figure 6). The voltage dependence of the lesion conductivity could only be determined from experiments in which the conductivities were constant over at least some seconds. Thus, the presence or absence of the voltage dependence of the lesion conductivity could only be determined in a small time interval before and after the change of the clamp voltage polarity (see inset of Figure 6).

Table 1: Summary of the Presented Microbiological and Biophysical Data[a]

	E. coli F515	*S. enterica* sv. Minnesota *R595*	*P. mirabilis* R45	human erythrocytes
antimicrobial/ hemolytic activity	+++	++	−	−[b]
interaction with monolayers	++	+	−	−
change of membrane capacitance	+++	+++	++	+
formation of membrane lesions	++	+	−	−

[a] (+++) high, (++) medium, (+) low, (−) non. [b] Taken from ref *14*.

DISCUSSION

In earlier studies, we could show that the activity of various AMPs against certain sensitive or resistant strains from different Gram-negative species as well as their cytotoxicity against eukaryotic cells is correlated with the lipid-specific interaction with the respective membranes (*19*−*23*). According to our findings, we hypothesize that the lipid-specificity of an AMP determines its biological activity. For all AMPs, either the permeabilization of the membrane or the passage through the membrane to reach their final locus of killing is essential. In the present study, we focused on the characterization of correlations between data obtained from biological assays and biophysical measurements on reconstituted membrane systems aiming at a deeper understanding of the molecular mechanisms of the biological activity of hBD3.

From antimicrobial assays using Gram-negative strains with a well-known structure of the LPS (Figure 1), we found that *P. mirabilis* strain R45 is resistant against hBD3, whereas *E. coli* strain F515 and *S. enterica* sv. Minnesota strain R595 are sensitive. Depending on the bacterial species, the antimicrobial activity of hBD3 shows a low salt sensitivity (*14*, *44*). Furthermore, no hemolytic activity of hBD3 against human erythrocytes has been found (*14*).

We prepared lipid monolayers using isolated LPS from the respective strains as the most simplified reconstitution system resembling the outer leaflet of the OM and, accordingly, PC for the reconstitution of the outer leaflet of the cytoplasmic membrane of eukaryotic cells. In film balance experiments, we found that hBD3 intercalates only into lipid monolayers made from LPS from the sensitive strains, but not into monolayers prepared of LPS R45 or PC (Table 1). The missing intercalation does not imply that binding of hBD3 to LPS R45 or PC monolayers can be excluded. In addition to the intercalation experiments, we prepared LB films of the respective monolayers and imaged them by the AFM technique to determine the influence of the peptide on membrane domain structures (Figure 2). Only in the case of LPS F515 and LPS R595 did we observe significant changes in domain structures of the LPS monolayers and the induction of new domains which probably contain or consist of hBD3. These effects demonstrate that hBD3 intercalates into the monolayer and induces a dramatic

change of the phase behavior and possibly also of the properties of the individual LPS molecules. One might speculate that the appearance of additional domains is due to an aggregation of hBD3 molecules in the monolayers which may be responsible for the formation of lesions and a decreased stability of the membranes. The lipid-specificity indicates that the lipid matrix plays an important role for the antimicrobial and the lack of hemolytic activity of hBD3. However, it cannot be excluded that other components of the bacterial cell wall or the eukaryotic membrane might also influence the interaction processes, in particular the formation of lesions or pores.

It has been shown that α- and insect defensins lead to increased membrane permeability in microbial, mammalian, and artificial membranes in a charge- or voltage-dependent manner. Moreover, α-defensins permeabilize both the outer and inner membranes of Gram-negative bacteria (*29*, *45*−*48*). To obtain information on the membrane permeabilizing activity of hBD3, we performed electrical measurements on planar lipid bilayers. We found that the addition of hBD3 to membranes with the leaflet directed toward peptide addition being composed of negatively charged PS or LPS led to changes in membrane capacitance of more than 10% (Figure 3, trace a); however, in the case of zwitterionic PC/PC membranes (Figure 3, trace b), a change of less than 5% even at a 10-fold higher peptide concentration was found. The change of the membrane capacitance can be due to peptide-induced changes of the membrane thickness or of the electrical properties of the membrane; therefore, on the basis of these data it is not possible to distinguish between the accumulation of the peptide on the membrane surface or the intercalation into the lipid matrix. From the fact that hBD3 leads to similar changes in the capacitance of all negatively charged membranes, it can be speculated that comparable amounts of peptide accumulate on the membrane surface. However, the film balance experiments showed that hBD3 does not intercalate into LPS R45 monolayers. The effect of hBD3 on membrane capacitance is small as compared to the effect we observed after addition of rabbit or human CAP18 fragments to the respective planar bilayers (*21*). This is consistent with the lower MIC values (higher potency) observed for the CAP18 fragments. Thus, it is likely that the depth of intercalation of hBD3 is lower and that more hBD3 molecules are needed to permeabilize the membranes. In contrast to the linear three-dimensional structure of CAP18 fragments, hBD3 has a globular character (*17*) and, thus, it may not be able to penetrate the membrane as deeply as α-helical peptides.

We found that hBD3 leads to the formation of transient lesions in LPS F515/PL and LPS R595/PL as well as in PS/PS and PS/PL membranes and, furthermore, causes destabilization of these membranes (Table 1). The induction of lesions strongly depends on the transmembrane voltage; they could only be induced at positive clamp voltages (corresponding to a transmembrane voltage being negative inside the cell). Interestingly, the voltage required for the induction of lesions in LPS/PL bilayers was <20 mV, i.e., lower than the transmembrane voltage (26 mV) across the OM of Gram-negative bacteria (*43*). Lesion formation and membrane destabilization were not observed for PC/PC and LPS R45/PL membranes (Figure 4, trace b). These results indicate that the lipid-specificity of hBD3 as observed for its intercalation into monolayers and in lesion formation experiments is an important descriptor for an understanding of its antimicrobial activity and the lack of its hemolytic activity. The influence of the clamp voltage on the orientation of the hBD3 molecules in the membranes and on the lesion formation is underlined by the observation that at negative clamp voltages hBD3-induced lesions had the tendency to close almost completely (Figures 5 and 6). This effect was more pronounced for phospholipid membranes than for LPS containing bilayers. This might be due to the formation of lesions which are more stable because of the binding of hBD3 to the more expanded region of negative charges in the headgroups of the LPS molecules. In contrast to other peptides, e.g., the amoebapores (*49*) or PMB (*37*), the lesions induced by hBD3 showed a heterogeneous distribution in size as well as in lifetime. A similar behavior was described earlier for fragments of human CAP18 (*21*). From our findings it can be deduced that hBD3 does not form pores of a defined geometry, but leads to a disturbance of membrane integrity by a process analogous to the carpet mechanism as described for phospholipid membranes (*50*, *51*). The dependence of the conductivity on the polarity of the applied voltage was observed for asymmetric LPS/PL but not for symmetric or asymmetric phospholipid bilayers (Figures 5 and 6). These observations allow us to conclude that the geometry of lesions formed in phospholipid bilayers is different from that in LPS/PL bilayers, indicating that the underlying mechanisms of lesion formation are different in the two membrane systems. The asymmetric voltage dependence of the conductivity may arise from an asymmetry in the geometry of the lesions or in the charge distribution in the lesions (*52*).

In the present study, we could show that *E. coli* strain F515, expressing an ReLPS not substituted by Ara4N (Figure 1), is sensitive to hBD3 (Table 1). The *S. enterica* sv. Minnesota strain R595, expressing an ReLPS which is substituted by Ara4N only on the 4′-phosphate of the first glucosamine, is also sensitive to hBD3. However, *P. mirabilis* strain R45, expressing an ReLPS with a second substitution by Ara4N on the first Kdo, is highly resistant to hBD3. One possibility is, thus, that a sterical hindrance by the second Ara4N on the first Kdo inhibits hBD3 from a deep intercalation into the membrane and, thus, from the formation of lesions. In earlier studies on planar lipid bilayers, we could show for fragments of the antimicrobial domains of human and rabbit CAP18, respectively, and for PMB that the positive charges of the peptide and the negative charge density of the lipid matrix on the side of peptide addition play an important role for their activities (*19*−*22*, *37*). Similar results have been described also for magainin-derived peptides in a calcein release assay (*53*). However, these cationic peptides exhibit an amphipathic α-helical or, in the case of PMB, a cyclic structure and are therefore not comparable to hBD3 which has a β-sheet structure with 6 cysteines in disulfide linkage. It may, nevertheless, be expected that also the interaction of the polycationic hBD3 with negatively charged membranes is driven by electrostatic forces. However, in the present study we found that differences in the sensitivity of Gram-negative bacteria cannot solely be explained by differences in the electrostatic interaction between hBD3 and the respective membranes. The assumption that the amount of Ara4N in the oligosac-

charide of the LPS is decisive for the depth of intercalation of hBD3 and with that for its antibacterial activity is further backed by the observation that the Gram-negative species *Burkholderia*, the LPS of which is highly substituted by Ara4N (*54*, *55*), is resistant against hBD3 (*18*). Besides sterical hindrance, also binding of certain antimicrobial peptides to the oligosaccharide of LPS can lead to the loss of their antimicrobial activity (*56*). However, the additional Ara4N linked to the first Kdo of LPS R45 is positively charged and hBD3 contains 13 positively and only 2 negatively charged side chains, and, therefore, electrostatic binding on the basis of the above cited mechanism is unlikely to occur.

The observation that the interaction between hBD3 and zwitterionic PC/PC membranes is negligible can explain the lack of hemolytic activity against eukaryotic cells (*14*). This is ascribable to the lack of electrostatic interactions with the headgroup of PC.

From the data presented in this paper, our hypothesis, that the biological activities of hBD3 against various targets are determined by lipid-specific interactions, could be verified. We do not exclude that also other factors, e.g., enzymes or proteins of the bacteria, might play additional roles in the killing mechanism. However, the permeation of the outer membrane of Gram-negative bacteria is the first essential step for hBD3 to reach its final locus of killing. Similar specificities caused by charges and/or sterical effects of certain functional groups of the lipid molecules, e.g., Ara4N on the Kdo of the LPS, have been found in earlier studies for other AMPs (*19*−*22*, *37*), indicating that lipid-specific interactions may be a general principle for the biological activities of a huge variety of AMPs.

We propose a four-step model for the interaction between hBD3 and membranes:

(i) The polycationic hBD3 accumulates in particular at negatively charged lipid surfaces, mainly driven by electrostatic forces.

(ii) The intercalation of hBD3 depends on electrostatic forces; however, the position of charged groups is decisive for the depth of intercalation. In particular, the positively charged Ara4N residue at the first Kdo of LPS from *P. mirabilis* strain R45 inhibits an intercalation into the membrane sufficiently deep to allow a disturbance of membrane integrity.

(iii) Depending on the lipid-specific intercalation depth of hBD3, lesions can be formed, probably by a "carpetlike" mechanism, and the membrane loses its overall stability. The AFM images are indicative for lesion formation by aggregation of hBD3 molecules in membranes. The voltage-dependent conductivity is lipid-specific, demonstrating that the lesion geometry is influenced by the chemical structure of the lipids. The lipid-specific effects leading to different intercalation depths or to different conductivities are not necessarily identical.

(iv) Ions and/or hBD3 can permeate through the membrane lesions. This self-promoted uptake (*37*, *57*) allows hBD3 to reach its final locus of killing.

ACKNOWLEDGMENT

We are indebted to Dr. Buko Lindner, Helga Lüthje, and Brigitte Kunz from the Research Center Borstel (Borstel, Germany) for mass spectrometric analysis of LPS used in this study and Sonja Hollmer for excellent technical assistance.

REFERENCES

1. Schröder, J. M. (1999) Epithelial peptide antibiotics, *Biochem. Pharmacol. 57*, 121−134.
2. Elsbach, P. (1998) The bactericidal/permeability-increasing protein (BPI) in antibacterial host defense, *J. Leukocyte Biol. 64*, 14−18.
3. Hirata, M., Zhong, J., Wright, S. C., and Larrick, J. W. (1995) Structure and functions of endotoxin-binding peptides derived from CAP18, *Prog. Clin. Biol. Res. 392*, 317−326.
4. Martin, E., Ganz, T., and Lehrer, R. I. (1995) Defensins and other endogenous peptide antibiotics of vertebrates, *J. Leukocyte Biol. 58*, 128−135.
5. Ganz, T., and Lehrer, R. I. (1998) Antimicrobial peptides of vertebrates, *Curr. Opin. Immunol. 10*, 41−44.
6. Gläser, R., Harder, J., Lange, H., Bartels, J., Christophers, E., and Schröder, J. M. (2005) Antimicrobial psoriasin (S100A7) protects human skin from *Escherichia coli* infection, *Nat. Immunol. 6*, 57−64.
7. Diamond, G., and Bevins, C. L. (1998) β-Defensins: endogenous antibiotics of the innate host defense response, *Clin. Immunol. Immunopathol. 88*, 221−225.
8. Bals, R., Wang, X., Zasloff, M., and Wilson, J. M. (1998) The peptide antibiotic LL-37/hCAP-18 is expressed in epithelia of the human lung where it has broad antimicrobial activity at the airway surface, *Proc. Natl. Acad. Sci. U.S.A 95*, 9541−9546.
9. Ganz, T., and Lehrer, R. I. (1995) Defensins, *Pharmacol. Ther. 66*, 191−205.
10. Lehrer, R. I., and Ganz, T. (2002) Defensins of vertebrate animals, *Curr. Opin. Immunol. 14*, 96−102.
11. Bensch, K. W., Raida, M., Mägert, H.-J., Schulz-Knappe, P., and Forssmann, W.-G. (1995) hBD-1: a novel β-defensin from human plasma, *FEBS Lett. 368*, 331−335.
12. Harder, J., Bartels, J., Christophers, E., and Schröder, J. M. (1997) A peptide antibiotic from human skin, *Nature 387*, 861.
13. Schröder, J. M., and Harder, J. (1999) Human beta-defensin-2, *Int. J. Biochem. Cell Biol. 31*, 645−651.
14. Harder, J., Bartels, J., Christophers, E., and Schröder, J. M. (2001) Isolation and characterization of human β-defensin-3, a novel human inducible peptide antibiotic, *J. Biol. Chem. 276*, 5707−5713.
15. Garcia, J. R. C., Krause, A., Schulz, S., Rodriguez-Jimenez, F. J., Klüver, E., Adermann, K., Forssmann, U., Frimpong-Boateng, A., Bals, R., and Forssmann, W. G. (2001) Human beta-defensin 4: a novel inducible peptide with a specific salt-sensitive spectrum of antimicrobial activity, *FASEB J. 15*, 1819−1821.
16. Tang, Y. Q., and Selsted, M. E. (1993) Characterization of the disulfide motif in BNBD-12, an antimicrobial β-defensin peptide from bovine neutrophils, *J. Biol. Chem. 268*, 6649−6653.
17. Schibli, D. J., Hunter, H. N., Aseyev, V., Starner, T. D., Wiencek, J. M., McCray, P. B., Jr., Tack, B. F., and Vogel, H. J. (2002) The solution structures of the human β-defensins lead to a better understanding of the potent bactericidal activity of HBD3 against Staphylococcus aureus, *J. Biol. Chem. 277*, 8279−8289.
18. Sahly, H., Schubert, S., Harder, J., Rautenberg, P., Ullmann, U., Schröder, J. M., and Podschun, R. (2003) *Burkholderia* is highly resistant to human β-defensin 3, *Antimicrob. Agents Chemother. 47*, 1739−1741.
19. Gutsmann, T., Larrick, J. W., Seydel, U., and Wiese, A. (1999) Molecular mechanisms of interaction of rabbit CAP18 with outer membranes of Gram-negative bacteria, *Biochemistry 38*, 13643−13653.
20. Gutsmann, T., Fix, M., Larrick, J. W., and Wiese, A. (2000) Mechanisms of action of rabbit CAP18 on monolayers and liposomes made from endotoxins or phospholipids, *J. Membr. Biol. 176*, 223−236.
21. Gutsmann, T., Hagge, S. O., Larrick, J. W., Seydel, U., and Wiese, A. (2001) Interaction of CAP18-derived peptides with membranes made from endotoxins or phospholipids, *Biophys. J. 80*, 2935−2945.
22. Hagge, S. O., Wiese, A., Seydel, U., and Gutsmann, T. (2004) Inner field compensation as a tool for the characterization of asymmetric membranes and peptide-membrane interactions, *Biophys. J. 86*, 913−922.

23. Wiese, A., Brandenburg, K., Carroll, S. F., Rietschel, E. T., and Seydel, U. (1997) Mechanisms of action of the bactericidal/permeability-increasing protein BPI on reconstituted outer membranes of Gram-negative bacteria, *Biochemistry 36*, 10311−10319.
24. Brötz, H., and Sahl, H. G. (2000) New insights into the mechanism of action of lantibiotics—diverse biological effects by binding to the same molecular target, *J. Antimicrob. Chemother. 46*, 1−6.
25. Vaara, M. (1992) Agents that increase the permeability of the outer membrane, *Microbiol. Rev. 56*, 395−411.
26. Nikaido, H., and Vaara, M. (1985) Molecular basis of bacterial outer membrane permeability, *Microbiol. Rev. 49*, 1−32.
27. Osborn, M. J., Gander, J. E., Parisi, E., and Carson, J. (1972) Mechanism and assembly of the outer membrane of *Salmonella typhimurium*, *J. Biol. Chem. 247*, 3962−3972.
28. Blodgett, K. B. (1935) Films built by depositing successive monomolecular layers on a solid surface, *J. Am. Chem. Soc. 57*, 1007−1022.
29. Kagan, B. L., Selsted, M. E., Ganz, T., and Lehrer, R. I. (1990) Antimicrobial defensin peptides form voltage-dependent ion-permeable channels in planar lipid bilayer membranes, *Proc. Natl. Acad. Sci. U.S.A. 87*, 210−214.
30. Wu, M., Maier, E., Benz, R., and Hancock, R. E. W. (1999) Mechanism of interaction of different classes of cationic antimicrobial peptides with planar bilayers and with the cytoplasmic membrane of *Escherichia coli*, *Biochemistry 38*, 7235−7242.
31. Montal, M., and Mueller, P. (1972) Formation of bimolecular membranes from lipid monolayers and a study of their electrical properties, *Proc. Natl. Acad. Sci. U.S.A. 69*, 3561−3566.
32. Seydel, U., Schröder, G., and Brandenburg, K. (1989) Reconstitution of the lipid matrix of the outer membrane of Gram-negative bacteria as asymmetric planar bilayer, *J. Membr. Biol. 109*, 95−103.
33. Zähringer, U., Lindner, B., Seydel, U., Rietschel, E. T., Naoki, H., Unger, F. M., Imoto, M., Kusumoto, S., and Shiba, T. (1985) Structure of de-O-acylated lipopolysaccharide from the *Escherichia coli* Re mutant strain F 515, *Tetrahedron Lett. 26*, 6321−6324.
34. Rietschel, E. T., Brade, L., Lindner, B., and Zähringer, U. (1992) Biochemistry of lipopolysaccharides, in *Bacterial Endotoxic Lipopolysaccharides, Vol. I: Molecular Biochemistry and Cellular Biology* (Morrison, D. C., and Ryan, J. L., Eds.) 1st ed., pp 3−41, CRC Press, Boca Raton.
35. Rietschel, E. T., Kirikae, T., Schade, F. U., Mamat, U., Schmidt, G., Loppnow, H., Ulmer, A. J., Zähringer, U., Seydel, U., Di Padova, F., Schreier, M., and Brade, H. (1994) Bacterial endotoxin: molecular relationships of structure to activity and function, *FASEB J. 8*, 217−225.
36. Vinogradov, E. V., Thomas-Oates, J. E., Brade, H., and Holst, O. (1994) Structural investigation of the lipopolysaccharide from *Proteus mirabilis* R45 (Re-chemotype), *J. Endotoxin Res. 1*, 199−206.
37. Wiese, A., Münstermann, M., Gutsmann, T., Lindner, B., Kawahara, K., Zähringer, U., and Seydel, U. (1998) Molecular mechanisms of Polymyxin B-membrane interactions: direct correlation between surface charge density and self-promoted uptake, *J. Membr. Biol. 162*, 127−138.
38. Holst, O. (1999) Chemical structure of the core region of lipopolysaccharides, in *Endotoxin in Health and Disease* (Brade, H., Opal, S. M., Vogel, S. N., and Morrison, D. C., Eds.) 1st ed., pp 115−154, Marcel Dekker, Inc., New York.
39. Galanos, C., Lüderitz, O., and Westphal, O. (1969) A new method for the extraction of R lipopolysaccharides, *Eur. J. Biochem. 9*, 245−249.
40. Marcelja, S. (1974) Chain ordering in liquid crystals II. Structure of bilayer membranes, *Biochim. Biophys. Acta 367*, 165−176.
41. Wiese, A., and Seydel, U. (2000) Electrophysiological measurements on reconstituted outer membranes, *Methods Mol. Biol. 145*, 355−370.
42. Shaw, N. (1974) Lipid composition as a guide to the classification of bacteria, *Adv. Appl. Microbiol. 17*, 63−108.
43. Sen, K., Hellman, J., and Nikaido, H. (1988) Porin channels in intact cells of *Escherichia coli* are not affected by Donnan potentials across the outer membrane, *J. Biol. Chem. 263*, 1182−1187.
44. Boniotto, M., Antcheva, N., Zelezetsky, I., Tossi, A., Palumbo, V., Verga Falzacappa, M. V., Sgubin, S., Braida, L., Amoroso, A., and Crovella, S. (2003) A study of host defence peptide β-defensin 3 in primates, *Biochem. J. 374*, 707−714.
45. Sawyer, J. G., Martin, N. L., and Hancock, R. E. W. (1988) Interaction of macrophage cationic proteins with the outer membrane of *Pseudomonas aeruginosa*, *Infect. Immun. 56*, 693−698.
46. Fujii, G., Selsted, M. E., and Eisenberg, D. (1993) Defensins promote fusion and lysis of negatively charged membranes, *Protein Sci. 2*, 1301−1312.
47. Cociancich, S., Ghazi, A., Hetru, C., Hoffmann, J. A., and Letellier, L. (1993) Insect defensin, an inducible antibacterial peptide, forms voltage-dependent channels in Micrococcus luteus, *J. Biol. Chem. 268*, 19239−19245.
48. Hristova, K., Selsted, M. E., and White, S. H. (1997) Critical role of lipid composition in membrane permeabilization by rabbit neutrophil defensins, *J. Biol. Chem. 272*, 24224−24233.
49. Gutsmann, T., Riekens, B., Bruhn, H., Wiese, A., Seydel, U., and Leippe, M. (2003) Interaction of amoebapores and NK-lysin with symmetric phospholipid and asymmetric lipopolysaccharide/phospholipid bilayers, *Biochemistry 42*, 9804−9812.
50. Oren, Z., Lerman, J. C., Gudmundsson, G. H., Agerberth, B., and Shai, Y. (1999) Structure and organization of the human antimicrobial peptide LL-37 in phospholipid membranes: relevance to the molecular basis for its non- cell-selective activity, *Biochem. J. 341*, 501−513.
51. Shai, Y. (1999) Mechanism of the binding, insertion and destabilization of phospholipid bilayer membranes by α-helical antimicrobial and cell non-selective membrane-lytic peptides, *Biochim. Biophys. Acta 1462*, 55−70.
52. Siwy, Z., and Fulinski, A. (2002) Fabrication of a synthetic nanopore ion pump, *Phys. Rev. Lett. 89*, 198103-1-198103-4.
53. Dathe, M., Nikolenko, H., Meyer, J., Beyermann, M., and Bienert, M. (2001) Optimization of the antimicrobial activity of magainin peptides by modification of charge, *FEBS Lett. 501*, 146−150.
54. Gronow, S., Noah, C., Blumenthal, A., Lindner, B., and Brade, H. (2003) Construction of a Deep-rough Mutant of *Burkholderia cepacia* ATCC 25416 and Characterization of Its Chemical and Biological Properties, *J. Biol. Chem. 278*, 1647−1655.
55. Isshiki, Y., Kawahara, K., and Zähringer, U. (1998) Isolation and characterisation of disodium (4-amino-4-deoxy-beta-L-arabinopyranosyl)-(1→8)-(D-glycero-alpha-D-talo-oct-2-ulopyranosylonate)-(2→4)-(methyl 3-deoxy-D-manno-oct-2-ulopyranosid)onate from the lipopolysaccharide of Burkholderia cepacia, *Carbohydr. Res. 313*, 21−27.
56. Papo, N., and Shai, Y. (2005) A molecular mechanism for lipopolysaccharide protection of Gram-negative bacteria from antimicrobial peptides, *J. Biol. Chem. 280*, 10378−10387.
57. Hancock, R. E. W. (1984) Alterations in outer membrane permeability, *Annu. Rev. Microbiol. 38*, 237−264.

BI052026E